

Supplementary Materials: The role of metal ions in the electron transport through azurin-based junctions

Carlos Romero-Muñiz^{1,2,3*} , María Ortega¹, J. G. Vilhena⁴ , Rubén Pérez^{1,5}  Juan Carlos Cuevas^{1,5}  and Linda A. Zotti^{1,3,5*} 

Contents

1 Parameters for inter-atomic interaction	2
2 MD simulation used for obtaining the metal-protein-metal geometries	5
3 Transmission curves for the Apo-azurin	6
References	7

1. Parameters for inter-atomic interaction

From Figures S1-S4, we detail the parameters used for describing the inter-atomic interaction between the three metal ions (Cu, Co, Ni) and its corresponding ligands on the azurin free solved in water MD simulations.

H46		H117		M121		C112		G45		Cu (II)	
atom	charge	atom	charge								
N	-0.68436	N	-0.55447	N	-0.51701	N	-0.58363	N	-0.54808	Cu	0.52457
H	0.30632	H	0.34433	H	0.36466	H	0.38982	H	0.34748		
C^a	0.50583	C^a	0.36957	C^a	0.17993	C^a	0.25509	C^a	0.19365		
H^a	0.0437	H^a	0.04198	H^a	0.05907	H^a	0.05485	H^{a2}	0.05056		
C^b	-0.30642	C^b	-0.36749	C^b	-0.17392	C^b	-0.03993	H^{a3}	0.0632		
H^{b2}	0.13339	H^{b2}	0.19163	H^{b2}	0.08436	H^{b2}	0.02367	C	0.53548		
H^{b3}	0.07175	H^{b3}	0.15248	H^{b3}	0.11801	H^{b3}	0.13984	O	-0.54122		
C^c	0.15265	C^c	0.22438	C^c	-0.04336	S^c	-0.49014				
N^{c1}	-0.11693	N^{c1}	-0.15728	H^{c2}	0.12755	C	0.36378				
C^{c1}	-0.08009	C^{c1}	-0.06305	H^{c3}	0.07229	O	-0.42484				
H^{c1}	0.14747	H^{c1}	0.13167	S^c	-0.3105						
N^{c2}	-0.09112	N^{c2}	-0.1354	C^c	-0.25136						
H^{c2}	0.33035	H^{c2}	0.33979	H^{c1}	0.10895						
C^{c2}	-0.25365	C^{c2}	-0.22283	H^{c2}	0.13454						
H^{c2}	0.21132	H^{c2}	0.20245	H^{c3}	0.10244						
C	0.2758	C	0.31687	C	0.28985						
O	-0.36587	O	-0.37736	O	-0.37706						

Figure S1. Partial charges for the metal coordination sphere used on the Cu-azurin free solved MD simulations.

H46		H117		M121		C112		G45		Co (II)	
atom	charge	atom	charge								
N	-0.59325	N	-0.52517	N	-0.5144	N	-0.55419	N	-0.53599	Co	0.54198
H	0.33634	H	0.34163	H	0.35152	H	0.37915	H	0.33499		
C ^a	0.27001	C ^a	0.33363	C ^a	0.24339	C ^a	0.22044	C ^a	0.14693		
H ^a	0.0993	H ^a	0.05301	H ^a	0.0473	H ^a	0.07691	H ^{a2}	0.06962		
C ^b	-0.39039	C ^b	-0.45632	C ^b	-0.27831	C ^b	-0.11389	H ^{a3}	0.08621		
H ^{b2}	0.16185	H ^{b2}	0.18314	H ^{b2}	0.15493	H ^{b2}	0.15425	C	0.49352		
H ^{b3}	0.11405	H ^{b3}	0.2712	H ^{b3}	0.11517	H ^{b3}	0.01771	O	-0.42529		
C ^c	0.41959	C ^c	0.25218	C ^c	-0.0125	S ^c	-0.57272				
N ^{d1}	-0.27555	N ^{d1}	-0.1964	H ^{c2}	0.10971	C	0.37047				
C ^{e1}	-0.11087	C ^{e1}	-0.06434	H ^{c3}	0.07165	O	-0.42166				
H ^{e1}	0.18069	H ^{e1}	0.16688	S ^e	-0.31527						
N ^{e2}	-0.02161	N ^{e2}	-0.17786	C ^e	-0.24338						
H ^{e2}	0.31876	H ^{e2}	0.34835	H ^{e1}	0.09641						
C ^{e2}	-0.40846	C ^{e2}	-0.17962	H ^{e2}	0.1179						
H ^{e2}	0.22759	H ^{e2}	0.17524	H ^{e3}	0.11598						
C	0.38134	C	0.3115	C	0.29624						
O	-0.3893	O	-0.37463	O	-0.39729						

Figure S2. Partial charges for the metal coordination sphere used on the Co-azurin free solved MD simulations.

H46		H117		M121		C112		G45		Ni (II)	
atom	charge	atom	charge								
N	-0.49918	N	-0.58642	N	-0.51052	N	-0.61445	N	-0.5403	Ni	0.41585
H	0.29056	H	0.36891	H	0.35328	H	0.39347	H	0.35739		
C ^a	0.23476	C ^a	0.36169	C ^a	0.1814	C ^a	0.26621	C ^a	0.18062		
H ^a	0.19302	H ^a	0.04399	H ^a	0.05601	H ^a	0.06903	H ^{a2}	0.07053		
C ^b	-0.35294	C ^b	-0.32486	C ^b	-0.143	C ^b	0.06839	H ^{a3}	0.08307		
H ^{b2}	0.15757	H ^{b2}	0.15084	H ^{b2}	0.11414	H ^{b2}	0.10616	C	0.39496		
H ^{b3}	0.10348	H ^{b3}	0.16935	H ^{b3}	0.08111	H ^{b3}	-0.00653	O	-0.39517		
C ^c	0.15976	C ^c	0.23558	C ^c	-0.12267	S ^c	-0.71044				
N ^{d1}	-0.08264	N ^{d1}	-0.07132	H ^{c2}	0.14162	C	0.33874				
C ^{e1}	-0.03455	C ^{e1}	-0.10609	H ^{c3}	0.07834	O	-0.42968				
H ^{e1}	0.13155	H ^{e1}	0.12702	S ^e	-0.25174						
N ^{e2}	-0.15163	N ^{e2}	-0.06919	C ^e	-0.29583						
H ^{e2}	0.34523	H ^{e2}	0.33172	H ^{e1}	0.13329						
C ^{e2}	-0.23187	C ^{e2}	-0.29851	H ^{e2}	0.1247						
H ^{e2}	0.20825	H ^{e2}	0.23192	H ^{e3}	0.12474						
C	0.37203	C	0.32288	C	0.2953						
O	-0.38067	O	-0.38088	O	-0.37738						

Figure S3. Partial charges for the metal coordination sphere used on the Ni-azurin free solved MD simulations.

Cu (II)			Co (II)			Ni (II)		
bond	r _{eq} (Å)	k _r (kcal/mol Å ²)	bond	r _{eq} (Å)	k _r (kcal/mol Å ²)	bond	r _{eq} (Å)	k _r (kcal/mol Å ²)
Cu-S ^γ (C112)	2,148	129	Co-S ^γ (C112)	2,193	127.8	Ni-S ^γ (C112)	2,211	110.9
Cu-N ^{δ1} (H46)	1,965	107,7	Co-N ^{δ1} (H46)	2,095	76,5	Ni-N ^{δ1} (H46)	2,038	80,4
Cu-N ^{δ1} (H117)	1,936	126,4	Co-N ^{δ1} (H117)	2,056	88,4	Ni-N ^{δ1} (H117)	1,966	120,4
Cu-O (G45)	2,76	5,6	Co-O (G45)	2,178	28,4	Ni-O (G45)	2,008	57,5
Cu-S ^δ (M121)	3,43	3,6	Co-S ^δ (M121)			Ni-S ^δ (M121)		

Figure S4. Bonded parameters within the metal coordination sphere. Bond distances and its corresponding force constants between the three metal ions (Cu, Co, Ni) and its corresponding ligands used on the azurin free solved MD simulations. Note that the amino acid M121 is directly bonded to the metal ion only for the Cu(II) case.

2. MD simulation used for obtaining the metal-protein-metal geometries

The metal-protein-metal geometries were obtained from prior MD simulations where a Cu-azurin adsorbed over a Au(111) slab is indented by a gold tip [1]. Such simulations were performed using AMBER14 software suite [2] with NVIDIA GPU acceleration [3–5]). The gold-azurin-gold junction consisted on a Au(111) surface where the protein was initially adsorbed and a Au(111) tip with 2 nm of radius that interacts with the adsorbed protein. The considered slab size is of $8 \times 8 \text{ nm}^2$ along the xy plane and three atomic layers-thick slab, with the positions of the bottom-most atoms restrained via an harmonic potential with a stiffness of 5 kcal/mol. The surface/tip gold atoms were described using CHARMM-METAL [6,7]. Previously we have shown that this potential is able to accurately describe structure, dynamics, and mechanical properties of both inorganic [8,9] and organic [10] molecules over Au(111). All standard azurin amino acids were described using the ff14SB force field [11] whilst the inter-atomic interactions between the copper atom and its corresponding 5 ligands were described using a quantum mechanically derived force field [12]. The X-ray crystallographic structure of azurin was obtained from the protein data bank with the PDB code 4AZU [13]. In order to reproduce prior experiments [14], the protonation state of the protein was set to a pH of 4.5. In all simulations, the junction is fully embedded in a water medium, where the solvent molecules are described using explicit TIP3P water-model [15].

The simulation protocol consisted of a two stage process: a) free adsorption of the azurin to an Au(111) surface; b) lateral indentation of the as adsorbed azurin with an Au(111) tip. In both cases: *i*) the energy of the structures was minimized; *ii*) the pressure was stabilized using a 1 ns long NPT simulation (all simulations are performed in liquid medium); and *iii*) the production runs were performed in the NVT ensemble. Regarding the free adsorption stage, the protein is initially positioned at 1 nm from the Au(111) surface and it is then allowed to freely adsorb to the surface (see Ref. 16 for more details). As for the lateral indentation stage, we start from the equilibrium configuration obtained from the previous stage (free adsorption). The gold tip (with the corresponding solvating water) is introduced at ~ 5.5 nm away from the azurin copper ion in the x direction. Then, we start to reduce the tip-protein distance by translating the tip at a velocity of 0.05 m/s in the x direction, i.e. parallel to one of the gold surface axis. When the protein and the tip are only separated by one hydration layer, we reduce the tip velocity to 0.025 m/s. Once the protein is firmly anchored to the tip, we reduce again the tip velocity up to 0.0125 m/s, see more details on ref. [1]. The difference between the z coordinates of the tip bottommost layer and the surface topmost layer is set to ~ 1.9 nm during the whole simulation.

3. Transmission curves for the Apo-azurin

In Figure S5, we show the transmission curves for the Apo-azurin at all four distances considered for Figure 3 of the main text.

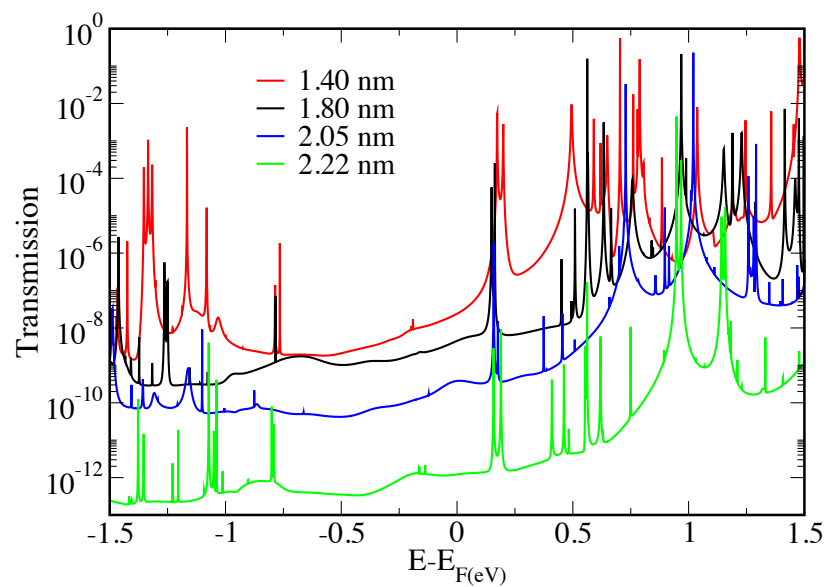


Figure S5. transmission as a function of energy for the Apo azurin at the four distance values considered for Figure 3 of the main text.

1. Romero-Muñiz, C.; Ortega, M.; Vilhena, J.G.; Díez-Pérez, I.; Pérez, R.; Cuevas, J.C.; Zotti, L.A. Can Electron Transport through a Blue-Copper Azurin Be Coherent? An Ab Initio Study. *J. Phys. Chem. C* **2021**, *125*, 1693–1702.
2. Case, D.A.; Darden, T.A.; III, T.E.C.; Simmerling, C.; Wang, J.; Duke, R.; Luo, R.; Walker, R.; Zhang, W.; Merz, K.; Roberts, B.; Hayik, S.; Roitberg, A.; Seabra, G.; Swails, J.; Götz, A.; Kolossváry, I.; Wong, K.; Paesani, F.; Vanicek, J.; Wolf, R.; Liu, J.; Wu, X.; Brozell, S.; Steinbrecher, T.; Gohlke, H.; Cai, Q.; Ye, X.; Wang, J.; Hsieh, M.J.; Cui, G.; Roe, D.; Mathews, D.; Seetin, M.; Salomon-Ferrer, R.; Sagui, C.; Babin, V.; Luchko, T.; Gusarov, S.; Kovalenko, A.; Kollman, P. AMBER 14, University of California, San Francisco, 2014. <http://ambermd.org/>.
3. Salomon-Ferrer, R.; Götz, A.W.; Poole, D.; Le Grand, S.; Walker, R.C. Routine Microsecond Molecular Dynamics Simulations with AMBER on GPUs. 2. Explicit Solvent Particle Mesh Ewald. *J. Chem. Theory Comput.* **2013**, *9*, 3878–3888.
4. Götz, A.W.; Williamson, M.J.; Xu, D.; Poole, D.; Le Grand, S.; Walker, R.C. Routine Microsecond Molecular Dynamics Simulations with AMBER on GPUs. 1. Generalized Born. *J. Chem. Theory Comput.* **2012**, *8*, 1542–1555.
5. Grand, S.L.; Götz, A.W.; Walker, R.C. SPFP: Speed without Compromise: A Mixed Precision Model for GPU Accelerated Molecular Dynamics Simulations. *Comput. Phys. Commun.* **2013**, *184*, 374–380.
6. Heinz, H.; Lin, T.J.; Kishore Mishra, Ratancand Emami, F.S. Thermodynamically Consistent Force Fields for the Assembly of Inorganic, Organic, and Biological Nanostructures: The INTERFACE Force Field. *Langmuir* **2013**, *29*, 1754–1765.
7. Heinz, H.; Ramezani-Dakhel, H. Simulations of Inorganic–Bioorganic Interfaces to Discover New Materials: Insights, Comparisons to Experiment, Challenges, and Opportunities. *Chem. Soc. Rev.* **2016**, *45*, 412–448.
8. Scherb, S.; Hinaut, A.; Pawlak, R.; Vilhena, J.G.; Liu, Y.; Freund, S.; Liu, Z.; Feng, X.; Müllen, K.; Glatzel, T.; Narita, A.; Meyer, E. Giant Thermal Expansion of a Two-Dimensional Supramolecular Network Triggered by Alkyl Chain Motion. *Commun. Mater.* **2020**, *1*, 8.
9. Pawlak, R.; Vilhena, J.G.; D'astolfo, P.; Liu, X.; Prampolini, G.; Meier, T.; Glatzel, T.; Lemkul, J.A.; Häner, R.; Decurtins, S.; Baratoff, A.; Pérez, R.; Liu, S.X.; Meyer, E. Sequential Bending and Twisting around C-C Single Bonds by Mechanical Lifting of a Pre-Adsorbed Polymer. *Nano Lett.* **2020**, *20*, 652–657.
10. Pawlak, R.; Vilhena, J.G.; Hinaut, A.; Meier, T.; Glatzel, T.; Baratoff, A.; Gnecco, E.; Pérez, R.; Meyer, E. Conformations and Cryo-Force Spectroscopy of Spray-Deposited Single-Strand DNA on Gold. *Nat. Commun.* **2019**, *10*, 685.
11. Maier, J.A.; Martinez, C.; Kasavajhala, K.; Wickstrom, L.; Hauser, K.E.; Simmerling, C. ff14SB: Improving the Accuracy of Protein Side Chain and Backbone Parameters from ff99SB. *J. Chem. Theory Comput.* **2015**, *11*, 3696–3713.
12. van den Bosch, M.; Swart, M.; Snijderst, J.G.; Berendsen, H.J.C.; Mark, A.E.; Oostenbrink, C.; van Gunsteren, W.F.; Canters, G.W. Calculation of the Redox Potential of the Protein Azurin and Some Mutants. *ChemBioChem* **2005**, *6*, 738.
13. Nar, H.; Messerschmidt, A.; Huber, R.; van de Kamp, M.; Canters, G.W. Crystal Structure Analysis of Oxidized *Pseudomonas aeruginosa* Azurin at pH 5.5 and pH 9.0: A pH-Induced Conformational Transition Involves a Peptide Bond Flip. *J. Mol. Biol.* **1991**, *221*, 765–772.
14. Ruiz, M.P.; Aragonès, A.C.; Camarero, N.; Vilhena, J.G.; Ortega, M.; Zotti, L.A.; Pérez, R.; Cuevas, J.C.; Gorostiza, P.; Díez-Pérez, I. Bioengineering a Single-Protein Junction. *J. Am. Chem. Soc.* **2017**, *139*, 15337–15346.
15. Jorgensen, W.L.; Chandrasekhar, J.; Madura, J.D.; Impey, R.W.; Klein, M.L. Comparison of Simple Potential Functions for Simulating Liquid Water. *J. Chem. Phys.* **1983**, *79*, 926–935.
16. Ortega, M.; Vilhena, J.G.; Zotti, L.A.; Díez-Pérez, I.; Cuevas, J.C.; Pérez, R. Tuning Structure and Dynamics of Blue Copper Azurin Junctions via Single Amino-Acid Mutations. *Biomolecules* **2019**, *9*, 611.